



Inhibition of human APE1 and MTH1 DNA repair proteins by dextran-coated γ -Fe₂O₃ ultrasmall superparamagnetic iron oxide nanoparticles

Erdem Coskun^{‡,1} , Neenu Singh^{‡,2} , Leona D Scanlan³ , Pawel Jaruga⁴ , Shareen H Doak⁵ , Miral Dizdaroglu⁴  & Bryant C Nelson^{*,6} 

¹Institute for Bioscience & Biotechnology Research, University of Maryland, Rockville, MD 20850, USA

²Leicester School of Allied Health Sciences, Faculty of Health & Life Sciences, De Montfort University, The Gateway, Leicester, LE1 9BH, UK

³California Environmental Protection Agency, Office of Environmental Health Hazard Assessment, 1001 I Street, Sacramento, CA 95814, USA

⁴Biomolecular Measurement Division, National Institute of Standards & Technology, Gaithersburg, MD 20899, USA

⁵Institute of Life Science, Center for NanoHealth, Swansea University Medical School, Wales, SA2 8PP, UK

⁶Biosystems & Biomaterials Division, National Institute of Standards & Technology, Gaithersburg, MD 20899, USA

*Author for correspondence: bryant.nelson@nist.gov

‡Authors contributed equally

Aim: To quantitatively evaluate the inhibition of human DNA repair proteins APE1 and MTH1 by dextran-coated γ -Fe₂O₃ ultrasmall superparamagnetic iron oxide nanoparticles (dUSPIONS). **Materials & methods:** Liquid chromatography–tandem mass spectrometry with isotope-dilution was used to measure the expression levels of APE1 and MTH1 in MCL-5 cells exposed to increasing doses of dUSPIONS. The expression levels of APE1 and MTH1 were measured in cytoplasmic and nuclear fractions of cell extracts. **Results:** APE1 and MTH1 expression was significantly inhibited in both cell fractions at the highest dUSPION dose. The expression of MTH1 was linearly inhibited across the full dUSPION dose range in both fractions. **Conclusion:** These findings warrant further studies to characterize the capacity of dUSPIONS to inhibit other DNA repair proteins *in vitro* and *in vivo*.

Plain language summary: Inhibitors of DNA repair proteins are increasingly being utilized as potential anticancer agents to supplement traditional chemotherapy and radiation-based approaches. The present study was focused on investigating the use of iron oxide nanoparticles to inhibit the expression of relevant human DNA repair proteins in a cellular model (MCL-5 cells). The authors utilized liquid chromatography–tandem mass spectrometry with isotope dilution to measure the expression levels of two different DNA repair proteins (MTH1 and APE1) in cells after the cells were exposed to increasing levels of the iron oxide nanoparticles. The authors observed significant decreases in DNA repair protein levels that were associated with increasing doses of the iron oxide nanoparticles. The authors' findings warrant more comprehensive studies using other cellular models and suitable animal models.

First draft submitted: 8 August 2022; Accepted for publication: 14 December 2022; Published online: 28 February 2023

Keywords: anticancer agents • APE1 • DNA repair protein inhibition • iron oxide nanoparticles • MTH1

Cancerous cells are examples of how rapid environmental and biological adaptation can result in accelerated cell evolution and cell death [1]. The primary aim of cancer treatments using chemotherapy and/or radiation therapy is to induce damage to the DNA of cancerous cells, ultimately leading to cell death. However, rapidly growing tumors accumulate mutations that lead to overexpression of DNA repair genes, which results in increased DNA repair capacity. Increased expression of DNA repair proteins in cancer cells is an important mechanism of cancer cell survival and resistance to anticancer therapy [2,3]. This increased production or enzymatic activity of DNA

repair proteins that removes DNA lesions before they can become toxic to the cell can also reduce the efficacy of anticancer drugs and ionizing radiation. There is mounting evidence that inhibitors of DNA repair proteins increase the efficiency of anticancer treatments by inhibiting the DNA repair-mediated removal of DNA lesions that are toxic to cancer cells. Hence, DNA repair pathways and select DNA repair proteins in these pathways, such as PARP1, APE1 and MTH1, have become promising targets for novel anticancer treatments [3]. PARP1 is an established sensor of cellular DNA damage and initiator of PARylation (synthesis of poly-ADP-ribosyl groups) [4]. APE1 is part of the base excision repair (BER) pathway and is singularly responsible for the removal of apurinic/aprimidinic sites [5]. MTH1 catalyzes the hydrolysis of modified dNTPs into monophosphates, preventing their incorporation into DNA by DNA polymerases during replication [6–8]. MTH1 has been shown to be required by cancer cells for survival by preventing the incorporation of modified dNTPs that would lead to cell death; therefore, it is a promising target in cancer therapy [9,10]. There are numerous ongoing clinical trials specifically focused on the application of small-molecule inhibitors of DNA repair proteins as anticancer agents (<https://clinicaltrials.gov>) [3,11–13]. Some of these compounds, such as PARP1 inhibitors olaparib, rucaparib and niraparib, have already been approved by the US FDA. Research on other small-molecule inhibitors that can potentially inhibit DNA repair proteins has gained tremendous traction in the last few years. Similar to PARP1 [13], APE1 [12,14,15] and MTH1 [16,17], DNA glycosylases have also become potential targets for selective inhibition in cancer treatment protocols [18].

An emerging technology for inhibiting the activity or expression of DNA repair proteins has focused on the use of engineered nanomaterials (ENMs). Certain types of ENMs can induce damage in nuclear DNA in the form of DNA adducts, oxidatively induced modifications and strand breaks under both acellular and cellular conditions [19,20]. These same ENMs can also potentially impair the enzymatic activity of DNA repair proteins [21,22]. Several types of ENMs, such as Ag nanoparticles [23], TiO₂ nanoparticles [24,25] and CuO nanoparticles [26], inhibit the activity of DNA repair proteins; CuO has been shown to specifically inhibit the DNA repair activity of PARP1 in an A549 (lung cancer) cell model. Ultrasmall superparamagnetic iron oxide nanoparticles (USPIONs) and superparamagnetic iron oxide nanoparticles (SPIONs) are ENMs based on either γ -Fe₂O₃ or Fe₃O₄ molecular structures that are increasingly being utilized in nanomedicine and drug delivery even though concerns have been raised about potential safety issues regarding their use in biomedical applications [27,28]. The authors' group has previously shown that dextran-coated γ -Fe₂O₃ USPIONs (dUSPIONs) have the capacity to form multiple oxidatively induced DNA lesions (e.g., 8-OH-Gua) in a human lymphoblastoid cell line (MCL-5) [29]. The mechanism of DNA lesion formation was demonstrated to be due to the intracellular release of Fe ions from the dUSPIONs. It was postulated that the released Fe ions underwent the Fenton reaction to produce reactive oxygen species such as the hydroxyl radical. The hydroxyl radical can efficiently induce oxidative damage in a variety of biomolecules, including proteins and DNA, under diffusion-controlled conditions. A correlation may exist between the induction of DNA damage by dUSPIONs and DNA repair protein inhibition by dUSPIONs.

Despite the potential adverse effects shown in various toxicity studies, USPIONs have been found to be unique targeted drug-delivery systems owing to their superparamagnetic properties. These drug-delivery systems allow the use of low therapeutic doses, as they can transport the drug directly into the tumor tissue (with the help of an external magnetic field), thus ameliorating the side effects of chemotherapy drugs [30]. The immense capability of USPIONs in nanomedicine has driven extensive efforts to design and optimize these materials to be effective therapeutic agents in cancer treatment. An important yet unanswered question is whether USPIONs can be utilized to affect or alter DNA repair pathways (e.g., inhibit DNA repair protein expression or activity) under experimentally controlled and quantitative conditions that may potentially result in the development of an additional tool in the fight against cancer.

Here the authors quantified the potential inhibitory effect of dUSPIONs on the endogenous expression levels of APE1 and MTH1 in MCL-5 cells. The structure and biological functions of the APE1 and MTH1 proteins in cancer treatment are well documented, but there is a paucity of accurate quantification of their levels in human tissues or cell lines. Measurement of DNA repair protein levels is predominantly based on western blotting or quantitative real-time PCR analyses [31–38]. Western blotting-based methods depend on antibodies, which may result in a false positive as a result of off-target binding of the antibodies. PCR analyses quantify RNA expression, not protein expression. An additional challenge is the inherently low endogenous levels (femtomole) of some DNA repair proteins in specific sample types (normal vs tumor cells) and selected sample compartments (nucleus vs cytoplasm), which requires that the quantification methods have a high analytical accuracy and sensitivity and a very low limit of detection. In the present study, the authors utilized liquid chromatography–tandem mass spectrometry (LC-MS/MS) with isotope dilution – a highly accurate and sensitive technique with a low detection

limit – to quantify the absolute expression levels of APE1 and MTH1 in the nuclear and cytoplasmic fractions of MCL-5 cells following exposure to increasing doses of dUSPIONS. Previously, the authors have shown that LC-MS/MS with isotope dilution provides positive identification and accurate quantification of APE1, MTH1 and PARP1 in cultured human cells and human disease-free and cancerous tissues [39–42]. Here the authors extend this methodology to provide quantitatively reproducible data on the inhibitory effects of dUSPIONS on the cellular expression of these proteins. The authors' approach is generally applicable to other biomedically relevant ENMs and will thus enable rigorous investigations on DNA repair proteins both within and outside of the BER pathway. Together, the analytical procedures and methods will ensure the quality, consistency and comparability of reported DNA repair protein levels, facilitating meaningful crosscomparison of results across laboratories. The data in the present study may potentially be aligned with existing data to extend our molecular and biological mechanistic understanding of DNA repair protein inhibition in order to develop improved anticancer modalities.

Materials & methods

Materials

dUSPIONS were purchased from Liquids Research Ltd (Bangor, UK). Roswell Park Memorial Institute (RPMI) 1640, horse serum, L-glutamine, sodium pyruvate and antibiotics were purchased from Thermo Fisher Scientific (Loughborough, UK). N-acetyl-L-cysteine, dimethyl sulfoxide, L-ascorbic acid sodium salt, ferrozine, pyridine and neocuproine were obtained from Sigma-Aldrich (Dorset, UK). The human lymphoblastoid cell line (MCL-5) was purchased from American Type Culture Collection/Gentest Corporation (MD, USA) and cultured in RPMI 1640 supplemented with 10% horse serum and 1% L-glutamine. Nitrilotriacetic acid disodium salt, FeCl₃, trypsin (proteomics grade), acetonitrile (HPLC grade), acetonitrile plus 0.1% formic acid (HPLC grade), water (HPLC grade), water plus 0.1% formic acid (HPLC grade) and trifluoroacetic acid (HPLC grade, ≥99%) were purchased from Sigma-Aldrich (MO, USA). The expression and purification of unlabeled human APE1, full-length fully ¹⁵N-labeled human APE1, unlabeled human MTH1 p18 isoform and full-length fully ¹⁵N-labeled human MTH1 were carried out as previously described [39,40,43–46]. The purity of all protein preparations was confirmed with SDS-PAGE and Coomassie staining. Distilled and deionized water (18.2 MΩ) was obtained from a Milli-Q system (MilliporeSigma, MA, USA) and used as indicated for all sample preparations.

Physicochemical characterization of dUSPIONS

The dUSPIONS utilized in this study were extensively characterized as described in previous studies [29,47,48].

Dynamic light scattering & zeta potential measurements

Hydrodynamic particle size measurements and ζ potential values of the dUSPIONS were determined using a 4700 spectrometer (Malvern Panalytical Ltd, Malvern, UK) and Zetasizer 2000 (Malvern Panalytical Ltd), respectively, as described previously [29]. For the analysis, dUSPIONS were dispersed in water or 1% serum and RPMI 1640 medium. The values presented are the average of ten readings.

x-ray photoelectron spectroscopy analysis

The oxidation state of the dUSPIONS, expressed as Fe²⁺-to-Fe³⁺ ratio, was confirmed by x-ray photoelectron spectroscopy as described previously [47].

Transmission electron microscopy analysis

Briefly, the MCL-5 cells treated with dUSPIONS were washed twice in serum-free medium and resuspended in 3% glutaraldehyde buffer solution for 2 h at 4°C followed by resuspension in 0.1% glutaraldehyde buffer as described previously [48]. The fixed cells were then processed for transmission electron microscopy analysis using an FEI/Philips CM200 (OR, USA) field emission gun and energy-dispersive x-ray detector. Example transmission electron microscopy data showing the uptake of dUSPIONS into MCL-5 cells are shown elsewhere [47].

Culture of MCL-5 cells & exposure to dUSPIONS

The MCL-5 cell line was cultured at 37°C with 5% CO₂ in RPMI 1640 medium supplemented with 10% horse serum and 1% L-glutamine. For the exposure studies, 1 × 10⁵ cells/ml were seeded for 24 h. The cells were then exposed to dUSPIONS at concentrations of 2, 4 or 10 μg/ml for 24 h in RPMI 1640 medium supplemented with 1% L-glutamine and 1% serum (test samples). Negative control cells (no dUSPION exposure) were prepared

identically to the dUSPION test samples. Positive control cells were prepared identically to the dUSPION test samples except that they were exposed to 10 mmol/l nitrilotriacetic acid disodium salt instead of dUSPIONs.

Cell viability measurements

Prior to frozen storage of the test samples, each sample was evaluated for cell viability on the basis of relative population doubling measurements as described previously [29]. There was no significant difference in the relative population doubling measurements for any of the test samples in comparison with the relative population doubling measurements for the negative control cells. Subsequently, the cells were washed twice in serum-free medium, resuspended in fresh serum-free medium and stored at -20°C for extraction of cytoplasmic and nuclear proteins. Three independently prepared samples were used for each data point.

Extraction of cytoplasmic & nuclear proteins & measurement of APE1 & MTH1

The protein fractions in each sample were extracted as described previously [42]. The amount of protein in the protein extracts was measured by the Bradford assay [49] using the Thermo Scientific Pierce Coomassie Protein Assay Kit (#23200; Thermo Fisher Scientific, IL, USA). An aliquot of ¹⁵N-labeled human APE1 or ¹⁵N-labeled human MTH1 was added to an aliquot (150 µg) of each protein extract followed by trypsin digestion [42]. The hydrolyzed protein extracts were analyzed by LC-MS/MS as described previously [39,40,42].

Statistical analysis

Three independently prepared DNA samples were used for each data point. Statistical analyses of the data were performed using Prism 8.4.3 software (GraphPad Software, CA, USA) with ordinary one-way analysis of variance and Tukey's multiple comparison tests.

Safety considerations

No unexpected, new or significant hazards or risks are associated with this study.

Results

Peptide profiling mass spectrometry analysis of MCL-5 cytoplasmic & nuclear protein extracts

The trypsin-hydrolyzed protein extracts from MCL-5 cells were analyzed with LC-MS/MS using selected reaction monitoring of the known tryptic peptides of APE1 and MTH1 and their fully ¹⁵N-labeled analogs ¹⁵N-labeled human APE1 and ¹⁵N-labeled human MTH1, respectively [39–41]. Four tryptic peptides (i.e., GF-GAGR, VQEGETIEDGAR, VLLGMK and FQGQDTILDYTLR) and their ¹⁵N-labeled analogs [40] were used for the identification and quantification of MTH1 in cytoplasmic and nuclear cell extracts. With 197 amino acids, these peptides constitute 18.8% of the sequence of MTH1. Nine tryptic peptides of APE1 (i.e., GLVR, TSPSGKPATLK, NAGFTPQER, NVGWR, GAVAEDGDELRL, WDEAFR, GLDWVK, EGYSGVGLLSR and QGFGELLQAVPLADSR) and their ¹⁵N-labeled analogs were used for the identification and quantification of APE1 [39]. With 318 amino acids, these peptides constitute 25.2% of the sequence of human APE1. According to the SwissProt.2021.06.18 database using the MS-Fit search (<https://prospector.ucsf.edu/prospector/cgi-bin/mform.cgi?form=msfitstandard>), any combination of just four tryptic peptides of MTH1 or APE1 provides 100% identification among the 565,254 entries in the database with the taxonomy search *Homo sapiens* (20,387 entries). This means that the simultaneous measurement of four tryptic peptides and their ¹⁵N-labeled analogs of MTH1 or APE1 provides positive identification and quantification of these proteins in protein extracts. Figure 1A & B illustrates examples of the mass-to-charge transitions of four tryptic peptides and their ¹⁵N-labeled analogs of MTH1 and APE1.

Measurement of MTH1 & APE1 expression levels in MCL-5 cytoplasmic & nuclear protein extracts

Measured levels of MTH1 are shown in Figure 2 for the cytoplasmic (Figure 2A) and nuclear (Figure 2B) fractions of MCL-5 cells before and after exposure to increasing doses of dUSPIONs. There was a distinctive dose-dependent inhibition of MTH1 expression levels in both the cytoplasmic and nuclear fractions. Compared with negative control levels, statistically significant dUSPION-induced inhibition of MTH1 expression was observed in the cytoplasmic fraction at 4 and 10 µg/ml ($p = 0.017$ and 0.0039 , respectively) (Figure 2A). In the nuclear fraction, there was also statistically significant inhibition of MTH1 expression at dUSPION concentrations of 4 and 10 µg/ml ($p = 0.0379$ and 0.0039 , respectively) (Figure 2B). Compared with negative control levels, a statistically

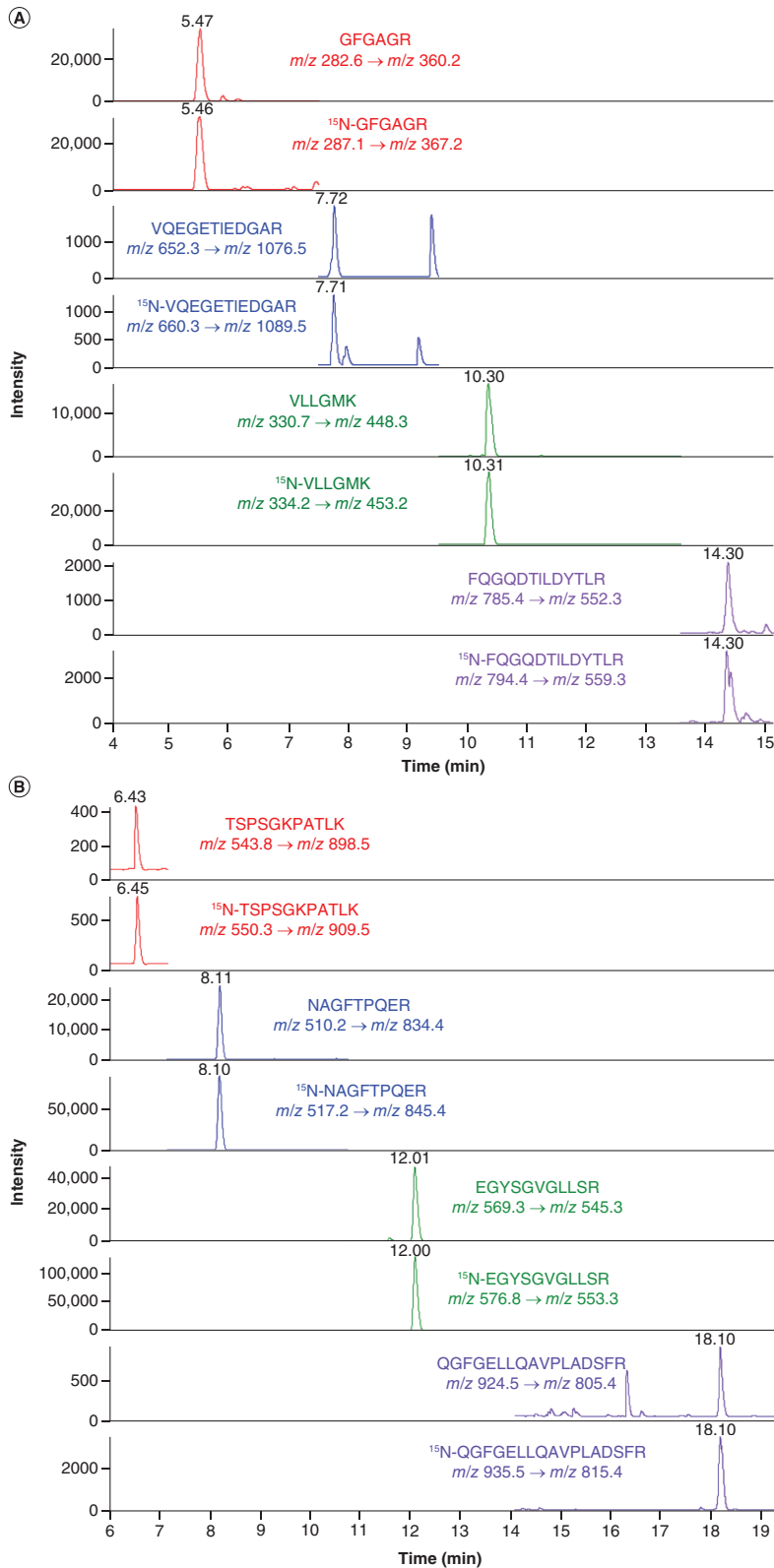


Figure 1. Characteristic ion current peptide profiles for MTH1 and APE1 DNA repair proteins extracted from MCL-5 cells. (A) Ion current profiles of m/z transitions of four tryptic peptides of MTH1 and their ¹⁵N-labeled analogs recorded using a cytoplasmic extract of MCL-5 cells. **(B)** Ion current profiles of m/z transitions of four tryptic peptides of APE1 and their ¹⁵N-labeled analogs recorded using a cytoplasmic extract of MCL-5 cells. m/z : Mass-to-charge.

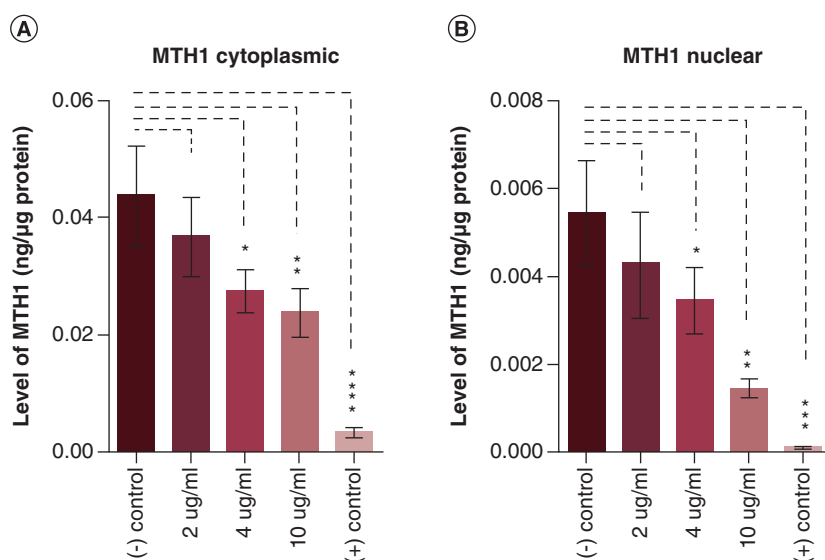


Figure 2. Liquid chromatography–tandem mass spectrometry measurement of MTH1 levels in MCL-5 cells exposed to dUSPIONS. Levels of MTH1 in (A) cytoplasmic and (B) nuclear extracts of MCL-5 cells exposed to increasing doses of dUSPIONS (2, 4 and 10 μg/ml). All data points represent the mean of the measurements of three independently prepared samples. Uncertainties are standard deviations.

* $p \leq 0.05$; ** $p \leq 0.01$; *** $p \leq 0.001$; **** $p \leq 0.0001$.

dUSPION: Dextran-coated γ - Fe_2O_3 ultrasmall superparamagnetic iron oxide nanoparticle.

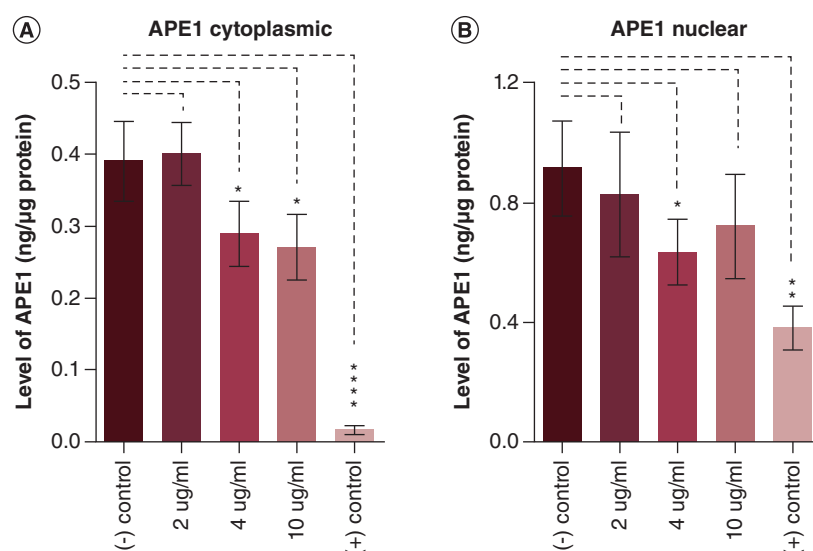


Figure 3. Liquid chromatography–tandem mass spectrometry measurement of APE1 levels in MCL-5 cells exposed to dUSPIONS. Levels of APE1 in (A) cytoplasmic and (B) nuclear extracts of MCL-5 cells exposed to increasing doses of dUSPIONS (2, 4 and 10 μg/ml). All data points represent the mean of the measurements of three independently prepared samples. Uncertainties are standard deviations.

* $p \leq 0.05$; ** $p \leq 0.01$; **** $p \leq 0.0001$.

dUSPION: Dextran-coated γ - Fe_2O_3 ultrasmall superparamagnetic iron oxide nanoparticle.

significant decrease in APE1 expression was observed in the cytoplasmic fraction with increasing dUSPION doses of 4 and 10 μg/ml ($p = 0.037$ and 0.045 , respectively) (Figure 3A). However, statistically significant inhibition ($p = 0.039$) of APE1 expression was observed in only the nuclear extracts (Figure 3B) at the dUSPION exposure level of 4 μg/ml. When negative control levels were compared with positive control levels for MTH1 and APE1, highly significant differences were observed ($p < 0.0001$ vs $p = 0.0035$) (Figure 2A & B & Figure 3A & B).

Discussion

Both SPIONs and USPIONs have been developed and widely utilized as therapeutic nanomedicine modalities in the treatment and diagnosis of cancers and other human-related pathologies [50–52]. For treatment purposes, small-molecule therapeutics are usually attached directly to either the core of the SPION or the biocompatible coating (e.g., polymer like dextran) surrounding the core. In terms of diagnostic applications, such as in vascular imaging, specific therapeutic agents do not necessarily need to be attached to the SPION core, as the superparamagnetic properties of the particles are the main components enabling their utility as sensitive contrast agents in MRI. SPION contrast agents are also effectively utilized for imaging tumors in lymph nodes and the liver. Current therapeutic and drug-delivery applications of SPIONs in cancer nanomedicine are geared toward their use in macrophage polarization, magnetic fluid hyperthermia and magnetic drug targeting [51]. Emerging areas in cancer theranostics incorporate SPIONs in image-guided drug delivery as well as the staging, diagnosis and treatment monitoring of cancers via magnetic-activated cell sorting [53].

Research on the inhibition of the expression or enzymatic activity of DNA repair proteins via interactions with SPIONs is sparse, but one early study demonstrated that iron ions (i.e., Fe^{2+}) can inhibit BER activity of the human DNA repair protein NEIL1 [54]. Using double-stranded oligodeoxynucleotides incorporating 5,6-dihydrouracil in a simple *in vitro* buffer model, the authors showed that Fe^{2+} inhibited the ability of human NEIL1 to remove the 5,6-dihydrouracil base from the oligodeoxynucleotides. The excision activity of human NEIL1 was most likely inhibited as a result of the formation of a metal ion–DNA complex that prevented the human NEIL1 from readily accessing the 5,6-dihydrouracil base. By contrast, Kain *et al.* recently showed that SPIONs had a negligible effect on the BER activity of bacterial DNA glycosylase *Escherichia coli* Fpg in A549 and BEAS-2B *in vitro* cell models [55]. The researchers utilized the comet assay to show that excision of the 8-hydroxyguanine from damaged DNA by *E. coli* Fpg was not significantly decreased in the presence of SPIONs. On the basis of this previous work, the effect of SPIONs on human DNA repair enzyme activity in cells and the mechanism through which it might occur remain unresolved.

Here the authors report a statistically significant inhibitory effect of dUSPIONs on the quantitative expression of both APE1 and MTH1 in the MCL-5 cell model. Following extraction, chromatographic isolation, purification and LC-MS/MS measurement of the characteristic tryptic peptides for each protein, the authors showed for the first time that dUSPIONs have a significant biological effect on the expression of DNA repair proteins in both the cytoplasmic and nuclear compartments of cells. Inhibition of APE1 and MTH1 protein expression was most evident at the highest dUSPION dose levels. Across the dUSPION dose levels utilized in the present study, the authors measured a clear inhibitory dose–response of MTH1 expression in the MCL-5 cytoplasmic and nuclear compartments. Cellular locations of the fully encoded proteins differ, with APE1 mainly localized in the nucleus [39,56,57] and MTH1 predominantly found in the cytoplasm [58,59]. The levels of APE1 and MTH1 measured in this work confirmed these previous findings, with the level of APE1 being greater in the nuclear fraction than in the cytoplasmic fraction (Figure 3), whereas the level of MTH1 was greater in the cytoplasmic fraction than in the nuclear fraction (Figure 2). The authors' results also indicate that native levels of the proteins in both cellular compartments differ (Figures 2 & 3). The background APE1 level (in the negative control sample) in the cytoplasmic compartments was approximately ten-times that of the MTH1 level. In the nuclear compartments, the difference was even more striking, with the background APE1 level (in the negative control sample) being approximately 180-times that of the MTH1 level. To the best of the authors' knowledge, in addition to our previous report on APE1 [39], the present work presents the only absolute identification and quantitative measurement of APE1 and MTH1 levels in cytoplasmic and nuclear locations in cell models [39–41].

Applicability & limitations

This short communication describes the 'indirect' cellular inhibition of two important human DNA repair proteins following exposure to well-characterized dUSPIONs. Based on highly precise mass spectrometry peptide profiles, the cellular expression of MTH1 and APE1 in both the cytoplasmic and nuclear compartments was measured and determined to be significantly inhibited at selected dUSPION dose levels. This type of quantitative analysis of protein expression using mass spectrometry peptide profiling should be amenable to the investigation of other types of both engineered (synthetic) and biological (e.g., extracellular vesicles) nanomaterials. Even though the observed results are provocative, the present study has some significant limitations. First, although the authors observed the uptake of dUSPIONs into the MCL-5 cells, the authors do not know for certain whether it was the activity of the dUSPIONs themselves or the potential activity of released Fe^{3+} ions (or perhaps both dUSPIONs and Fe^{3+}) that

was the main inhibitor of the observed DNA repair protein expression levels. Second, the study was not designed to evaluate the molecular or biological mechanisms that potentiate the inhibition of DNA repair protein expression levels. Hence, the authors are not able to establish whether it was the potential binding of the dUSPIONs or of the Fe^{3+} ions to the active sites on the MTH1 or APE1 DNA repair proteins or whether either the dUSPIONs or the Fe^{3+} ions inhibited expression of the DNA repair protein mRNA. Third, tandem mass spectrometry peptide profiling using isotope-labeled protein standards is a robust, analytically sensitive measurement approach for identifying and measuring low level proteins. The present study would have been even stronger if the authors had obtained data using an orthogonal measurement technique (e.g., isotope-coded affinity tag LC-MS/MS) to confirm expression levels of the reported DNA repair proteins. Finally, because this was a screening experiment to determine whether peptide profiling mass spectrometry would be a suitable quantitative method for evaluating dUSPION inhibition of DNA repair protein expression levels *in vitro*, the authors utilized a small number of independent biological samples ($n = 3$) for each dUSPION exposure level. For a more comprehensive study that would facilitate a more thorough characterization of the biological variation in DNA repair protein expression levels, it is recommended that the number of analyzed samples be increased ($n > 3$).

Conclusion

New therapeutic agents that selectively inhibit the DNA repair capacity of cancer cells could be excellent additions to the current cancer treatment arsenal of radiation therapy, immunotherapy and chemotherapy. The authors' finding that dUSPIONs inhibit DNA repair enzymes offers the possibility that targeted approaches for disrupting DNA repair pathways and inhibiting the enhanced DNA repair capacity of cancer cells can be achieved through next-generation ENMs such as exosome-encapsulated dUSPIONs [60,61] combined with high-affinity chemical inhibitors.

Summary points

- Inhibition of selected DNA repair proteins in cancerous cells using nanoparticles is a potential approach to cancer treatment that may complement or enhance the efficacy of traditional chemotherapy agents or radiation treatment modalities.
- This study quantitatively evaluated the ability of dextran-coated $\gamma\text{-Fe}_2\text{O}_3$ ultrasmall superparamagnetic iron oxide nanoparticles (dUSPIONs) to inhibit the cellular expression of the MTH1 and APE1 human DNA repair proteins in a lymphoblastoid (MCL-5) cell model.
- MCL-5 cell samples (1×10^5 cells/ml) were exposed to increasing dUSPION doses (2, 4 and 10 $\mu\text{g/ml}$) for 24 h.
- Cytoplasmic and nuclear protein extracts were collected and analyzed for the MTH1 and APE1 target proteins via liquid chromatography–tandem mass spectrometry with isotope dilution.
- Measurements were conducted on the characteristic tryptic peptides for each repair protein and DNA repair protein levels were calculated on the basis of tryptic peptide calibration curves.
- Dose-dependent inhibition of MTH1 expression levels in both the cytoplasmic and nuclear fractions was induced by exposure to the dUSPIONs.
- The most statistically significant decrease in MTH1 expression occurred at the 10- $\mu\text{g/ml}$ dUSPION dose ($p = 0.0039$) in both the cytoplasmic and nuclear fractions.
- Dose-dependent inhibition of APE1 expression levels was not observed.
- The most statistically significant decreases in APE1 expression occurred at the 10- $\mu\text{g/ml}$ dUSPION dose ($p = 0.045$) in the cytoplasmic fraction and at the 4- $\mu\text{g/ml}$ dUSPION dose ($p = 0.039$) in the nuclear fraction.
- The inhibition of human DNA repair proteins via dUSPIONs is observable and measurable using liquid chromatography–tandem mass spectrometry with isotope dilution; the capacity of dUSPIONs to potentially serve as effective anticancer agents warrants more comprehensive investigation and further validation studies in additional *in vitro* and *in vivo* systems.

Open access

This work is licensed under the Attribution-NonCommercial-NoDerivatives 4.0 Unported License. To view a copy of this license, visit <http://creativecommons.org/licenses/by-nc-nd/4.0/>

Disclosure

Certain commercial equipment or materials are identified in this article to specify the experimental procedure adequately. Such identification does not imply recommendation or endorsement by the National Institute of Standards and Technology, nor does it imply that the equipment or materials identified are necessarily the best available for the purpose.

Financial & competing interests disclosure

The authors have no relevant affiliations or financial involvement with any organization or entity with a financial interest in or financial conflict with the subject matter or materials discussed in the manuscript. This includes employment, consultancies, honoraria, stock ownership or options, expert testimony, grants or patents received or pending or royalties.

No writing assistance was utilized in the production of this manuscript.

Ethical conduct of research

The human cell line (MCL-5) was obtained from a commercial vendor (American Type Culture Collection/Gentest Corporation). All experiments were reviewed and approved by the National Institute of Standards and Technology Research Protections Office (project no. MML-16-0034).

References

Papers of special note have been highlighted as: ● of interest; ●● of considerable interest

1. Tang D, Kang R, Berghe TV, Vandenabeele P, Kroemer G. The molecular machinery of regulated cell death. *Cell Res.* 29(5), 347–364 (2019).
2. Gavande NS, Vandervere-Carozza PS, Hinshaw HD *et al.* DNA repair targeted therapy: the past or future of cancer treatment? *Pharmacol. Ther.* 160, 65–83 (2016).
3. Kelley MR, Fishel ML. *DNA Repair in Cancer Therapy, Molecular Targets and Clinical Applications*. Elsevier, Amsterdam, The Netherlands (2016).
- **Provides a comprehensive overview of present and future applications of DNA repair protein targeting in cancer therapy.**
4. Chaudhuri AR, Nussenzweig A. The multifaceted roles of PARP1 in DNA repair and chromatin remodelling. *Nat. Rev. Mol. Cell Biol.* 18(10), 610–621 (2017).
5. Wallace SS, Murphy DL, Sweasy JB. Base excision repair and cancer. *Cancer Lett.* 327(1–2), 73–89 (2012).
- **Provides a detailed understanding of the base excision repair pathway, which includes various enzymatic reactions important for DNA repair, includes various enzymatic reactions important for DNA repair proteins, including APE1, and highlights the importance of APE1 and other key enzymes as cancer therapy targets.**
6. Sakumi K, Furuichi M, Tsuzuki T *et al.* Cloning and expression of cDNA for a human enzyme that hydrolyzes 8-oxo-dGTP, a mutagenic substrate for DNA synthesis. *J. Biol. Chem.* 268(31), 23524–23530 (1993).
7. Kakuma T, Nishida J, Tsuzuki T, Sekiguchi M. Mouse MTH1 protein with 8-oxo-7,8-dihydro-2'-deoxyguanosine 5'-triphosphatase activity that prevents transversion mutation. cDNA cloning and tissue distribution. *J. Biol. Chem.* 270(43), 25942–25948 (1995).
8. Cai JP, Kakuma T, Tsuzuki T, Sekiguchi M. cDNA and genomic sequences for rat 8-oxo-dGTPase that prevents occurrence of spontaneous mutations due to oxidation of guanine nucleotides. *Carcinogenesis* 16(10), 2343–2350 (1995).
9. Huber KV, Salah E, Radic B *et al.* Stereospecific targeting of MTH1 by (S)-crizotinib as an anticancer strategy. *Nature* 508(7495), 222–227 (2014).
10. Gad H, Koolmeister T, Jemth AS *et al.* MTH1 inhibition eradicates cancer by preventing sanitation of the dNTP pool. *Nature* 508(7495), 215–221 (2014).
11. Sadiq MT, Madhusudan S. Evolving DNA repair targets for cancer therapy. In: *DNA Damage, DNA Repair and Disease: Volume 2*. Dizdaroglu M, Lloyd RS (Eds). Royal Society of Chemistry, Cambridge, UK, 254–285 (2021).
12. Gampala S, Caston RA, Fishel ML, Kelley MR. Basic, translational and clinical relevance of the DNA repair and redox signaling protein APE1 in human diseases. In: *DNA Damage, DNA Repair and Disease: Volume 2*. Dizdaroglu M, Lloyd RS (Eds). Royal Society of Chemistry, Cambridge, UK, 286–318 (2021).
13. Curtin NJ. The role of PARP and the therapeutic potential of PARP inhibitors in cancer. In: *DNA Damage, DNA Repair and Disease: Volume 2*. Dizdaroglu M, Lloyd RS (Eds). Royal Society of Chemistry, Cambridge, UK, 319–360 (2021).
14. Poletto M, Malfatti MC, Dorjsuren D *et al.* Inhibitors of the apurinic/apyrimidinic endonuclease 1 (APE1)/nucleophosmin (NPM1) interaction that display anti-tumor properties. *Mol. Carcinog.* 55(5), 688–704 (2016).
15. Caston RA, Gampala S, Armstrong L, Messmann RA, Fishel ML, Kelley MR. The multifunctional APE1 DNA repair–redox signaling protein as a drug target in human disease. *Drug Discov. Today* 26(1), 218–228 (2021).
- **Discusses the implication of APE1 in cancer and many other diseases because of its critical role in regulating key transcription factors.**
16. Puigvert JC, Sanjiv K, Helleday T. Targeting DNA repair, DNA metabolism and replication stress as anti-cancer strategies. *FEBS J.* 283(2), 232–245 (2016).
17. van der Waals LM, Laoukili J, Jongen JMJ, Raats DA, Borel Rinkes IHM, Kranenburg O. Differential anti-tumour effects of MTH1 inhibitors in patient-derived 3D colorectal cancer cultures. *Sci. Rep.* 9(1), 819 (2019).

18. McCullough AK, Minko IG, Nilsen A, Nagarajan S, Lloyd RS. Modulation of DNA glycosylase activities via small molecules. In: *DNA Damage, DNA Repair and Disease: Volume 2*. Dizdaroglu M, Lloyd RS (Eds). Royal Society of Chemistry, Cambridge, UK, 323–347 (2021).
19. Petersen EJ, Nelson BC. Mechanisms and measurements of nanomaterial-induced oxidative damage to DNA. *Anal. Bioanal. Chem.* 398(2), 613–650 (2010).
20. Singh N, Manshian B, Jenkins GJ *et al.* NanoGenotoxicology: the DNA damaging potential of engineered nanomaterials. *Biomaterials* 30(23–24), 3891–3914 (2009).
21. Carriere M, Sauvaigo S, Douki T, Ravanat JL. Impact of nanoparticles on DNA repair processes: current knowledge and working hypotheses. *Mutagenesis* 32(1), 203–213 (2017).
22. Singh N, Nelson BC, Scanlan LD, Coskun E, Jaruga P, Doak SH. Exposure to engineered nanomaterials: impact on DNA repair pathways. *Int. J. Mol. Sci.* 18(7), (2017). <http://dx.doi.org/10.3390/ijms18071515>
23. Wojewodzka M, Lankoff A, Dusinska M *et al.* Treatment with silver nanoparticles delays repair of x-ray induced DNA damage in HepG2 cells. *Nukleonika* 56(1), 29–33 (2011).
24. Armand L, Tarantini A, Beal D *et al.* Long-term exposure of A549 cells to titanium dioxide nanoparticles induces DNA damage and sensitizes cells towards genotoxic agents. *Nanotoxicology* 10(7), 913–923 (2016).
25. Jugan ML, Barillet S, Simon-Deckers A *et al.* Titanium dioxide nanoparticles exhibit genotoxicity and impair DNA repair activity in A549 cells. *Nanotoxicology* 6(5), 501–513 (2012).
26. Semisch A, Ohle J, Witt B, Hartwig A. Cytotoxicity and genotoxicity of nano- and microparticulate copper oxide: role of solubility and intracellular bioavailability. *Part. Fibre Toxicol.* 11, 10 (2014).
27. Singh N, Jenkins GJ, Asadi R, Doak SH. Potential toxicity of superparamagnetic iron oxide nanoparticles (SPION). *Nano Rev.* 1 (2010). <http://dx.doi.org/10.3402/nano.v1i0.5358>
28. Laurent S, Saei AA, Behzadi S, Panahifar A, Mahmoudi M. Superparamagnetic iron oxide nanoparticles for delivery of therapeutic agents: opportunities and challenges. *Expert Opin. Drug Deliv.* 11(9), 1449–1470 (2014).
29. Singh N, Jenkins GJ, Nelson BC *et al.* The role of iron redox state in the genotoxicity of ultrafine superparamagnetic iron oxide nanoparticles. *Biomaterials* 33(1), 163–170 (2012).
- **First known study to indicate that the oxidation state of iron in dextran-coated γ -Fe₂O₃ ultrasmall superparamagnetic iron oxide nanoparticles can modulate cellular uptake and genotoxicity in the absence of cytotoxicity.**
30. Fouzia NA, Sharma V, Ganesan S *et al.* Management of relapse in acute promyelocytic leukaemia treated with up-front arsenic trioxide-based regimens. *Br. J. Haematol.* 192(2), 292–299 (2021).
31. Chantre-Justino M, Alves G, Britto C *et al.* Impact of reduced levels of APE1 transcripts on the survival of patients with urothelial carcinoma of the bladder. *Oncol. Rep.* 34(4), 1667–1674 (2015).
32. Dietrich AK, Humphreys GI, Nardulli AM. 17 β -estradiol increases expression of the oxidative stress response and DNA repair protein apurinic endonuclease (Ape1) in the cerebral cortex of female mice following hypoxia. *J. Steroid Biochem. Mol. Biol.* 138, 410–420 (2013).
33. Kim YJ, Kim D, Illuzzi JL *et al.* S-glutathionylation of cysteine 99 in the APE1 protein impairs abasic endonuclease activity. *J. Mol. Biol.* 414(3), 313–326 (2011).
34. Lou D, Zhu L, Ding H, Dai HY, Zou GM. Aberrant expression of redox protein APE1 in colon cancer stem cells. *Oncol. Lett.* 7(4), 1078–1082 (2014).
35. Ma H, Wang J, Abdel-Rahman SZ, Boor PJ, Khan MF. Induction of base excision repair enzymes NTH1 and APE1 in rat spleen following aniline exposure. *Toxicol. Appl. Pharmacol.* 267(3), 276–283 (2013).
36. Meisenberg C, Tait PS, Dianova II *et al.* Ubiquitin ligase UBR3 regulates cellular levels of the essential DNA repair protein APE1 and is required for genome stability. *Nucleic Acids Res.* 40(2), 701–711 (2012).
37. Poletto M, Di Loreto C, Marasco D *et al.* Acetylation on critical lysine residues of apurinic/aprimidinic endonuclease 1 (APE1) in triple negative breast cancers. *Biochem. Biophys. Res. Commun.* 424(1), 34–39 (2012).
38. Xu J, Husain A, Hu W, Honjo T, Kobayashi M. APE1 is dispensable for S-region cleavage but required for its repair in class switch recombination. *Proc. Natl Acad. Sci. USA* 111(48), 17242–17247 (2014).
39. Kirkali G, Jaruga P, Reddy PT *et al.* Identification and quantification of DNA repair protein apurinic/aprimidinic endonuclease 1 (APE1) in human cells by liquid chromatography/isotope-dilution tandem mass spectrometry. *PLOS ONE* 8(7), e69894 (2013).
40. Coskun E, Jaruga P, Jemth AS *et al.* Addiction to MTH1 protein results in intense expression in human breast cancer tissue as measured by liquid chromatography–isotope-dilution tandem mass spectrometry. *DNA Repair (Amst.)* 33, 101–110 (2015).
41. Coskun E, Jaruga P, Reddy PT, Dizdaroglu M. Extreme expression of DNA repair protein apurinic/aprimidinic endonuclease 1 (APE1) in human breast cancer as measured by liquid chromatography and isotope dilution tandem mass spectrometry. *Biochemistry* 54(38), 5787–5790 (2015).

42. Coskun E, Tuna G, Jaruga P, Tona A, Erdem O, Dizdaroglu M. Identification and quantification of DNA repair protein poly(ADP ribose) polymerase 1 (PARP1) in human tissues and cultured cells by liquid chromatography/isotope-dilution tandem mass spectrometry. *DNA Repair (Amst.)* 75, 48–59 (2019).
43. Reddy PT, Jaruga P, Nelson BC, Lowenthal M, Dizdaroglu M. Stable isotope-labeling of DNA repair proteins, and their purification and characterization. *Protein Expr. Purif.* 78(1), 94–101 (2011).
44. Erzberger JP, Barsky D, Schärer OD, Colvin ME, Wilson DM III. Elements in abasic site recognition by the major human and *Escherichia coli* apurinic/apyrimidinic endonucleases. *Nucleic Acids Res.* 26(11), 2771–2778 (1998).
45. Svensson LM, Jemth AS, Desroses M *et al.* Crystal structure of human MTH1 and the 8-oxo-dGMP product complex. *FEBS Lett.* 585(16), 2617–2621 (2011).
46. Reddy PT, Jaruga P, Nelson BC *et al.* Production, purification, and characterization of ¹⁵N-labeled DNA repair proteins as internal standards for mass spectrometric measurements. *Methods Enzymol.* 566, 305–332 (2016).
47. Griffiths SM, Singh N, Jenkins GJ *et al.* Dextran coated ultrafine superparamagnetic iron oxide nanoparticles: compatibility with common fluorometric and colorimetric dyes. *Anal. Chem.* 83(10), 3778–3785 (2011).
48. Hondow N, Harrington J, Brydson R *et al.* STEM mode in the SEM: a practical tool for nanotoxicology. *Nanotoxicology* 5(2), 215–227 (2011).
49. Bradford MM. A rapid and sensitive method for the quantitation of microgram quantities of protein utilizing the principle of protein–dye binding. *Anal. Biochem.* 72, 248–254 (1976).
50. Boyer C, Whittaker MR, Bulmus V, Liu JQ, Davis TP. The design and utility of polymer-stabilized iron-oxide nanoparticles for nanomedicine applications. *NPG Asia Mater.* 2(1), 23–30 (2010).
51. Dadfar SM, Roemhild K, Drude NI *et al.* Iron oxide nanoparticles: diagnostic, therapeutic and theranostic applications. *Adv. Drug Deliv. Rev.* 138, 302–325 (2019).
52. Mahmoudi M, Sant S, Wang B, Laurent S, Sen T. Superparamagnetic iron oxide nanoparticles (SPIONs): development, surface modification and applications in chemotherapy. *Adv. Drug Deliv. Rev.* 63(1–2), 24–46 (2011).
53. Mi Y, Li K, Liu Y, Pu K-Y, Liu B, Feng S-S. Herceptin functionalized polyhedral oligomeric silsesquioxane – conjugated oligomers – silica/iron oxide nanoparticles for tumor cell sorting and detection. *Biomaterials* 32(32), 8226–8233 (2011).
54. Grin IR, Konorovsky PG, Nevinsky GA, Zharkov DO. Heavy metal ions affect the activity of DNA glycosylases of the FPG family. *Biochemistry (Mosc.)* 74(11), 1253–1259 (2009).
55. Kain J, Karlsson HL, Moller L. DNA damage induced by micro- and nanoparticles – interaction with FPG influences the detection of DNA oxidation in the comet assay. *Mutagenesis* 27(4), 491–500 (2012).
56. Tell G, Damante G, Caldwell D, Kelley MR. The intracellular localization of APE1/Ref-1: more than a passive phenomenon? *Antioxid. Redox Signal.* 7(3–4), 367–384 (2005).
57. Illuzzi JL, Wilson DM III. Base excision repair: contribution to tumorigenesis and target in anticancer treatment paradigms. *Curr. Med. Chem.* 19(23), 3922–3936 (2012).
58. Kang D, Nishida J, Iyama A *et al.* Intracellular localization of 8-oxo-dGTPase in human cells, with special reference to the role of the enzyme in mitochondria. *J. Biol. Chem.* 270(24), 14659–14665 (1995).
59. Nakabeppu Y. Regulation of intracellular localization of human MTH1, OGG1, and MYH proteins for repair of oxidative DNA damage. *Prog. Nucleic Acid Res. Mol. Biol.* 68, 75–94 (2001).
- **Describes the regulation of intracellular localization of human MTH1 protein for the repair of oxidatively induced DNA damage; in the present work, the authors measured the expression and inhibition of MTH1 protein in both cytoplasmic and nuclear compartments of a cellular model.**
60. Busato A, Bonafede R, Bontempi P *et al.* Magnetic resonance imaging of ultrasmall superparamagnetic iron oxide-labeled exosomes from stem cells: a new method to obtain labeled exosomes. *Int. J. Nanomed.* 11, 2481–2490 (2016).
61. Ailuno G, Baldassari S, Lai F, Florio T, Caviglioli G. Exosomes and extracellular vesicles as emerging theranostic platforms in cancer research. *Cells* 9(12), 2569 (2020).